Journal of Electroceramics, 14, 113–118, 2005

Effect of Rare Earth Europium Substitution on the Microstructure, Dielectric, Ferroelectric and Pyroelectric Properties of PZT Ceramics

RAJNI KHAZANCHI,* SEEMA SHARMA & T.C.GOEL

Advanced Ceramics Laboratory, Department of Physics, Indian Institute of Technology, New Delhi 110016, India

Submitted January 8, 2004; Revised August 3, 2004; Accepted August 10, 2004

Abstract. Polycrystalline samples of Europium modified lead Zirconate titanate $(Pb_{1-x}\,Eu_x)(Zr_{0.55}Ti_{0.45})_{(1-x/4)}O_3$ with $x = 0.00, 0.02, 0.04, 0.06$ has been prepared by mixed oxide (MO) method at sintering temperature of 1250°C. The structural characterization of the samples investigated by X-ray diffraction technique exhibit tetragonal structure. PEZT (2/55/45) ceramics show single perovskite phase. Scanning electron micrographs depict uniform, densely packed structure. Dielectric, Pyroelectric and Ferroelectric studies have been performed and are reported and discussed in this paper. PEZT (2/55/45) show good current responsivity (F_i), voltage responsivity (F_v) and detectivity (F_d), in comparison to other compositions under study. Moreover its ferroelectric properties (high remanent polarization with low coercive field) make it suitable material for nonvolatile memory applications.

Keywords: PZT, pyroelectric properties, ferroelectric properties

1. Introduction

Recently there has been a great interest in the field of electro ceramics for their ability to exhibit ferroelectric behaviour. Ferroelectric ceramics are being widely used in the Industrial applications such as thermal detectors, thermal imaging, high dielectric capacitors, computer memory and display, transducers and sensors [1–6].

$Pb(Zr_xTi_{1-x})O_3$ (PZT) are perovskite type ferroelectrics. Ceramics of PZT solid solutions are well known for their excellent piezoelectric and pyroelectric properties. The crystal structure and ferroelectric properties depend strongly on the composition. PZT solid solutions display a morphotropic phase boundary around $x = 0.54$ corresponding to a transition from a tetragonal to a rhombohedral structure.

The composition of Lead Zirconate Titanate ($PbZrTiO_3$) and substitution of rare earth doping i.e., La, Gd, Sm, Nd, has been studied for their excellent dielectric, pyroelectric, piezoelectric & electro optic properties and have been reported to improve and optimize their basic properties for wider applications [7–13]. Very little work has been reported on Europium modified PZT bulk ceramics [7].

Attempts have been made in the present work to investigate the microstructure, dielectric, ferroelectric and pyroelectric properties of rare earth Europium modified PZT ceramics.

2. Experimental

The rare earth Europium has been substituted in different proportions in PZT using chemical formula $(Pb_{1-x}Eu_x)(Zr_{0.55}Ti_{0.45})_{(1-x/4)}O_3$ wherein $x = 0.00$, 0.02, 0.04, 0.06. These ceramic samples are designated as PEZT 0, PEZT 2, PEZT 4, and PEZT 6 respectively. This substitution has been assumed to occupy vacancies in the A site (Pb position) so that the structure would be electrically neutral. The ceramics were prepared by mixed oxide (MO) method [5]. The starting precursors were Lead Oxide (PbO), Europium Oxide (Eu_2O_3), Titanium Oxide (TiO_2), Zirconium Oxide (ZrO_2), procured from Aldrich chemicals USA with purity of 99.999%. These oxides were mixed in stoichiometric proportions, and extra lead oxide (4% by weight) was added to the mixture for preventing lead loss during calcination and sintering processes. The

*Corresponding author. E-mail: rajnikhazanchi@vsnl.net

powders were mixed and ball milled with Zirconia balls for approx. 4 hours in an acetone medium. After drying the powders were calcined at 850°C in a furnace for 2 hours. Polyvinyl alcohol (4% by weight) was added as a binder to the calcined powder. The calcined mixture was then pulverized using a mortar and pestle and dried in air. The cylindrical pallets of 10 mm diameter and 1 mm thickness were formed by pressing the calcined powder in a hydraulic press using punch and die, under the load of 10 tons. These pellets were sintered at 1250°C for 2 hours in a closed alumina crucible in lead rich atmosphere.

X-ray diffraction was done on each sample of different composition on an X-ray diffractogram machine (Philips PW 1730/10) using Cu Kα radiation of $\lambda = 1.5418$ Å.

Surface electron microscopy using Cambridge Stereo Scan 360 equipment, was carried out to evaluate the grain size of the pellets. Silver electrodes were coated on these for investigating the electrical properties. Variation of dielectric constant and dielectric loss was measured as a function of temperature at different frequencies (0.1 kHz–1 MHz) using 4284A HP LCR meter. Hysteresis studies were carried out on electroded samples using Sawyer Tower circuit coupled with computer interfaced loop tracer.

The electroded samples were corona poled with a corona voltage of 5 kV at a current of 50 μA, for 15 minutes while heating the sample to 100°C, and then for 15 minutes while cooling the sample to room temperature. Corona poling was done to prevent electric breakdown of the samples. Pyro electric measurements were taken after corona poling. The pyro electric current was measured after 3rd heating cycle beyond which ceramic samples exhibit reproducible values of the current. This was measured at the heating rate of 3°C/min using the Keithley 610 C electrometer. Pyroelectric coefficient was calculated using the formula $Pi = (I/A)(dT/dt)^{-1}$ where I is the Pyro electric current in amperes measured after 3rd heating cycle; A is the elecroded area of the sample and dT/dt is the heating rate of the furnace.

3. Results and Discussions

3.1. Structural Studies

Figure 1 shows the XRD pattern of pure and doped PZT sintered samples. All compositions possess tetragonal

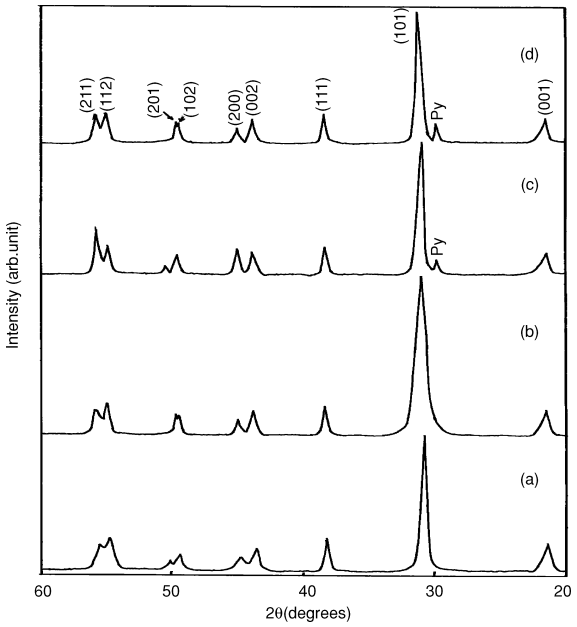

Fig. 1. XRD patterns of (a) PEZT 0, (b) PEZT 2, (c) PEZT 4 and (d) PEZT 6.

structure shown by well-resolved peaks at (002), (200), (201), (102), (211), (112) planes. PEZT 0 and PEZT 2 show single perovskite phase, while a small amount of pyrochlore phase is observed in PEZT 4 & PEZT 6 indicated as Py in Fig. 1(c) and (d), which is approx. 11% & 13% respectively as calculated using the formula:

$$\text{Pyrochlore } \% = (\text{Ipyro})/(\text{Ipyro} + \text{Iperov}) \times 100.$$

Shennigrahi et al. [7] suggested the possibilities of presence of pyrochlore phase in Eu doped PZT with $x = 0.08$.

Table 1 shows lattice parameter values of pure and doped PZT samples.

It is observed that the basic crystal structure of PZT is not affected by the substitution of Eu^{3+} and remains

Table 1. Lattice parameters of pure and doped PZT ceramics

Composition	Structure	c/a	Lattice volume (Å)^3	Experimental density	Average grain size (μm)
PEZT 0	Tetragonal	1.0314	68.22	7.47	2.60
PEZT 2	Tetragonal	1.0074	69.18	7.80	**2.00**
PEZT 4	Tetragonal	1.0280	67.80	7.19	1.25
PEZT 6	Tetragonal	1.0282	66.85	7.17	2.00

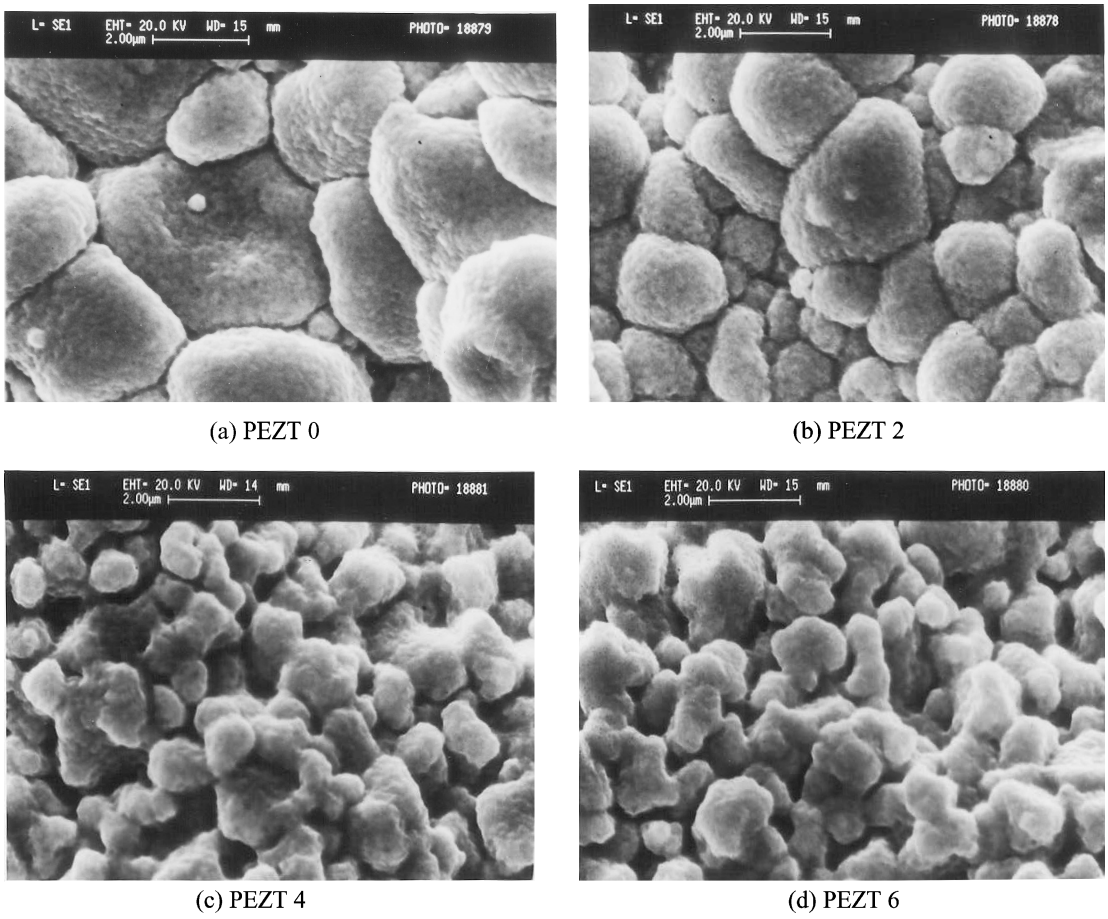

(a) PEZT 0 (b) PEZT 2

(c) PEZT 4 (d) PEZT 6

Fig. 2. (a)–(d): SEM photographs of pure and doped PZT ceramics.

tetragonal for all the compositions. For PEZT 2, c/a has decreased and increment in density and average grain size has been observed. However with increase in Eu concentration for $x = 0.04$ & 0.06, increase in c/a ratio and decrease in unit cell volume & bulk density is observed. This could be due to possibility of lead vacancies created due to incorporation of offvalent ion Eu^{3+} in place of Pb^{2+}. A decrease in bulk density with increasing La content in PLZT for all Zr to Ti ratios has also been reported by Haertling and Land [8].

SEM micrographs of the fractured ceramic samples are shown in Fig. 2(a)–(d). It is found that well developed grains are observed in all the compositions. PEZT 0 and PEZT 2 show uniform, densely packed, spherical in shape & crack free grains at the surface with no visible porosity, whereas in samples of PEZT 4 and PEZT 6, grain size are densely packed with few pores/islands present but seem to decrease in size. Grain size has been measured by linear intercept technique and is given in Table 1.

3.2. Dielectric Studies

Figure 3(a) shows variation in dielectric constant ε at 1 kHz frequency as a function of temperature for all compositions. Figure 3(b) shows dielectric loss at 1 kHz as a function of temperature for all compositions. It is observed that the variation in the dielectric constant and dielectric loss ($\tan\delta$) for all compositions remain almost constant up to 150°C, and then it starts increasing with increase in temperature till it reaches its curie temperature (T_c). The frequency dependence of the dielectric constant for all compositions shows

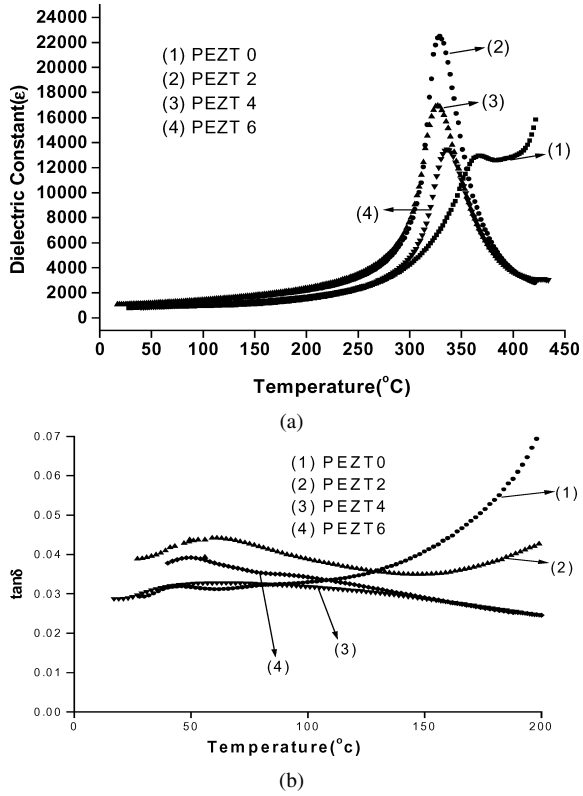

Fig. 3. (a): Variation of ε with temperature at 1 kHz. (b): Variation of tanδ with temperature at 1 kHz.

typical dielectric behaviour as seen in most ferroelectric materials. The values of dielectric constant and dielectric losses have been given in Table 2, measured at 100 Hz and 1 kHz.

Sharp decrease in c/a has been observed in PEZT 2 sample, which could lead to ease of 90° domain orientations thereby increasing dielectric constant [14]. Further with increase of Eu concentration ($x = 0.04$, 0.06), the tetragonality of the structure has increased, leading to reduction of the dielectric constant. This is also supported by the fact that the decrease in grain size for PEZT 4 and PEZT 6 leads to impediment to the domain wall mobility offered by the defects or the space charges [15, 16].

Table 2. Dielectric values of pure & doped PZT ceramics at room temperature

Composition	ε (100 Hz)	tanδ (100 Hz)	ε (1 kHz)	tanδ (1 kHz)	T_c (°C)
PEZT 0	858	0.04	814	0.03	366
PEZT 2	1205	0.04	1132	0.04	329
PEZT 4	1172	0.03	1118	0.03	327
PEZT 6	907	0.03	856	0.04	338

3.3. Ferroelectric Properties

Polarization vs. Electric field Hysteresis loops for pure and doped PZT ceramics are shown in Fig. 4.

Values of saturation polarization (P_s), remanent polarization (P_r) and coercive field (E_c) have been given in Table 3. Beginning from PZT pure, it is observed that P_r, P_s & E_c has increased with 2% Eu and 4% Eu, doping.

The higher value of P_s, P_r & E_c as compared to undoped PZT ceramics can be attributed to Pb vacancies formed due to Eu ion substitution. These Pb vacancies are negatively charged and these get paired with Eu^{+3} ions to form defect poles. These defect poles can be aligned when there is spontaneous polarization or when there is an applied electric field. This creates a larger polarization & hence can explain why doped PZT has larger P_r & P_s then undoped PZT, as observed in our samples [17]. Also sharp decrease of P_r and increase of E_c in PEZT 6 sample can be attributed to decrease in grain size [18].

The high values of P_r with low E_c in PEZT 2 sample show suitability of this material for nonvolatile memory applications.

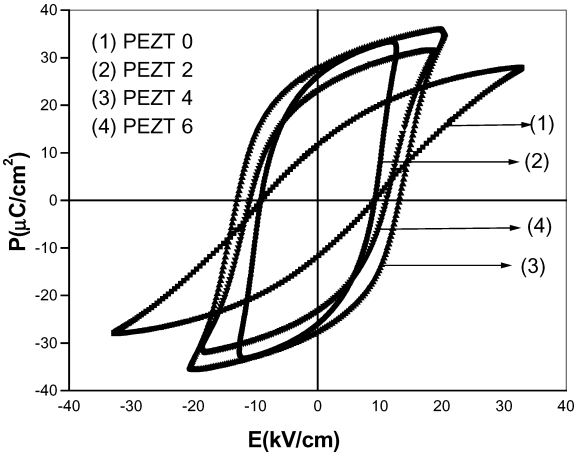

Fig. 4. Polarization—Electric field curve of pure and doped PZT ceramics.

Table 3. Pyroelectric properties of PEZT ceramics.

Composition	P_s (μC/cm^2)	P_r (μC/cm^2)	E_c (kV/cm)	P_i (μC/m^2 K)	$F_i\,x$ 10^{-8} (Cm/J)	F_v (m^2/C)		$F_d \times 10^{-6}$ (m^3/J)$^{1/2}$	
						100 Hz	1 kHz	100 Hz	1 kHz
PEZT 0	28.00	11.72	9.11	159	0.64	0.008	0.008	3.7	4.2
PEZT 2	33.26	26.05	9.17	420	1.70	0.016	0.017	8.1	8.4
PEZT 4	35.74	27.67	13.05	173	0.69	0.006	0.007	3.9	3.9
PEZT 6	31.73	18.71	11.00	153	0.61	0.008	0.008	3.9	3.6

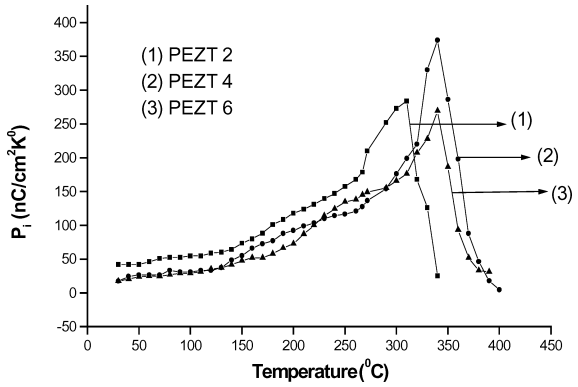

Fig. 5. Variation of pyrocoefficient with temperature.

3.4. Pyroelectric Properties

Variation of pyrocoefficient with temperature for pure and doped PZT ceramics is shown in Fig. 5.

Table 3 above, shows pyroelectric values for doped PZT ceramics. The appropriate figures of merit for pyroelectric materials are current responsivity (F_i), voltage responsivity (F_v) and detectivity (F_d), which have been calculated and given in Table 3.

It is found that PEZT 2 has highest pyrocoefficient at room temperature and hence the current responsivity is also high as compared to other PEZT compositions thus making it more responsive of these materials for use in detectors [19]. Also voltage responsivity and detectivity is observed good in case of PEZT 2 samples.

Also PEZT 2 bulk samples show very good pyroelectric figures of merit in comparison to the already studied bulk ceramics, PZT doped with La, Sm, Eu, Gd and Yb [20].

From the Fig. 5 and Fig. 3(a) and (b), we can see that pyroelectric coefficient, dielectric constant and loss tangent is almost uniform over the temperature range of 20°C to 150°C, so that the responsivity and detectivity of a detector made from this material would essentially be independent of the temperature and therefore can be operated over a wide range of temperature [21].

4. Conclusions

Rare earth Europium doped PZT ceramics with various concentration, have been studied for its structural, dielectric, ferroelectric and pyroelectric properties. The results are as mentioned below:

All ceramics with different concentrations show tetragonal structure. Pure PZT sample and PEZT 2 sample sintered at 1250°C show single perovskite structure whereas PEZT 4 and PEZT 6 samples sintered at 1250°C show pyrochlore phase. All compositions show typical dielectric behaviour. SEM micrographs show grains of micron size. The best Pyro current and Pyro coefficient is seen in PEZT 2/55/45. The best pyroelectric figures of merit have been observed in PEZT 2 composition. Therefore, this material can be used for infrared detectors, which can be operated over the temperature range of 20°C to 150°C.

Due to its high remanent polarization with a low coercive field, PEZT 2/55/45 can be considered potential material for nonvolatile memory applications.

References

1. M.E. Lines and A.M. Glass, *Principals and Applications of Ferroelectrics and Related Materials* (Oxford University Press, Oxford, 1977).
2. J.M. Herbert, *Ceramic Dielectric and Capacitors* (Gordon And Breach Science Publishers, New York, 1985).
3. L.E. Cross, *Jpn. J. Appl. Phys.*, **34**, 2525 (1995).
4. G.H. Haertling, *Ferroelectrics*, **75**, 25 (1987).
5. G.H. Haertling, *J. Am. Ceram. Soc.*, **82**, 4, 797 (1999).
6. R.W. Whatmore, *Rep. Prog. Phys.*, **49**, 1335 (1986).
7. S.R. Shanningrahi, F.E.H. Tay, K. Yao, and R.N.P. Choudhary, *Journal of European Ceramic Society*, **24**, 163 (2004).

8. G.H. Haertling and C.E. Land, *J. Am. Ceram. Soc.*, **54**(1) (1971).
9. Q. Wei Hng and H. Hoon, *Mater. Chem. and Phys*., **75**, 151 (2002).
10. S.R. Shanningrahi, R.N.P. Choudhary, and H.N. Acharya, *Mat. Sci. Eng. B-Solid*, **60**, 31 (1990).
11. S.R. Shanningrahi and R.N.P. Choudhary, *J. Electro-Ceram*, **5**, 201 (2000).
12. A. Garg and D.C. Agrawal, *Mater. Sci. and Eng. B*, **86**, 134 (2001).
13. A. Govindan, H.D. Sharma, A.K. Tripathi, P.K.C. Pillai, and T.C. Goel, *Ferroelectrics*, **134**, 217 (1992).
14. S.B. Mah, N.W. Jang, J.H. Park, D.S. Paik, and C.Y. Park, *Mat. Res. Bull.*, **35**, 1113 (2003)
15. K. Okazaki and K. Nagata, *J. Am. Ceram. Soc*., **82**, 56 (1973).
16. M. Takahashi, *Japn. J. Appl. Phys.*, **9**, 1236 (1970).
17. W. Qiu and H. H. Hng, *Materials Chemistry and Physics*, **75**, 151.
18. P. Muralt, *IEEE Trans*., UFFC 903 (2000).
19. K.K. Deb, *Ferroelectrics*, **88**, 167 (1988).
20. T.C. Goel, P.K.C. Pillai, H.D. Sharma, A.K. Tripathi, A. Tripathi, C. Pramilla, and Anil Govindan, in *Proc. 8th Int. Conf. on Electret(ISE -8) Paris*, 720 (1994).
21. K.K. Deb, *Ferroelectrics*, **82**, 45 (1988).